

See discussions, stats, and author profiles for this publication at: <http://www.researchgate.net/publication/258569390>

# Group III–Nitrides Nanostructures

ARTICLE *in* AIP CONFERENCE PROCEEDINGS · FEBRUARY 2012

DOI: 10.1063/1.3678628

DOWNLOADS

76

VIEWS

81

## 9 AUTHORS, INCLUDING:



**I. Martínez-Velis**

Center for Research and Advanced Studies of...

10 PUBLICATIONS 8 CITATIONS

SEE PROFILE



**Salvador Gallardo**

Center for Research and Advanced Studies of...

32 PUBLICATIONS 39 CITATIONS

SEE PROFILE



**B. J. Babu**

Madanapalle Institute of Technology & Science

15 PUBLICATIONS 50 CITATIONS

SEE PROFILE



**Velumani S**

Center for Research and Advanced Studies of...

128 PUBLICATIONS 718 CITATIONS

SEE PROFILE



### **Group III-nitrides nanostructures**

M. Pérez-Caro, M. Ramírez-López, J. S. Rojas-Ramírez, I. Martínez-Velis, Y. Casallas-Moreno, S. Gallardo-Hernández, B. J. Babu, S. Velumani, and M. López-López

Citation: *AIP Conference Proceedings* **1420**, 164 (2012); doi: 10.1063/1.3678628

View online: <http://dx.doi.org/10.1063/1.3678628>

View Table of Contents: <http://scitation.aip.org/content/aip/proceeding/aipcp/1420?ver=pdfcov>

Published by the [AIP Publishing](#)

---

# Group III-Nitrides Nanostructures

M. Pérez-Caro<sup>a</sup>, M. Ramírez-López<sup>a</sup>, J.S. Rojas-Ramírez<sup>a</sup>, I. Martínez-Velis<sup>a</sup>, Y. Casallas-Moreno<sup>a</sup>, S. Gallardo-Hernández<sup>a</sup>, B. J. Babu<sup>b</sup>, S. Velumani<sup>b</sup>, and M. López-López<sup>a</sup>

<sup>a</sup>*Departamento de Física, Centro de Investigación y Estudios Avanzados del IPN, Apdo. Postal 14-740, México D.F. 07000, México.*

<sup>b</sup>*Solid-State Electronic Section, Department of Electrical Engineering, Centro de Investigación y Estudios Avanzados del IPN, Apartado Postal 14-740, México D.F. 07000, México.*

**Abstract.** We report on the growth and characterization of self-assembled InGaN columnar nanostructures grown by gas source molecular beam epitaxy (GSMBE) on Si(111) substrates. At a zero concentration of Ga, InN nanocolumns (NCs) were successfully grown. In the case of InGaN, the surface morphology is dependent on composition; however, in general, InGaN samples exhibit columnar features. At concentrations near 50%, the samples show phase separation; this result is explained in terms of solid phase immiscibility.

**Keywords:** Nanocolumns, Nitrides, Molecular Beam Epitaxy

**PACS:** 61.05.jh, 61.05.cp, 61.46.-w, 68.37.Hk, 81.07.-b, 81.16.-c

## INTRODUCTION

Group III-nitrides semiconductors family and related alloys have become a topic of great interest due to the many potential applications that could be realized from infrared (IR) up to deep ultraviolet (UV); including the entire visible region. In particular, it has been demonstrated that using InGaN ternary alloy, it is possible to tune the wavelength emission from IR to near-UV [1]; making this alloy very important in optoelectronic devices such as light emitting diodes [2,3], semiconductor lasers [4], solid-state lighting [5] and solar cells[6]. However, there are several constraints in order to obtain high quality InGaN films. The lack of native -or nearly-lattice matched substrates, the low dissociation temperature of InN ( $\sim 550$  °C) and the high growth temperature of GaN have been the main challenges in growing high quality InGaN material. An attempt for solving that issue is based on growing self-assembled nanostructures. That possibility allows having, in principle, a material with exceptional high crystal quality, free of defects and strain fields; ideal for studying the fundamental physical properties hindered in common highly defective InGaN films. It is well known, in GaN and InN binary compounds, that the growth of good quality films is performed under slightly metal-rich conditions; and, on the other hand, the growth under strong nitrogen-rich (N-rich) conditions results in columnar nanostructures. Based on the latter statement, we present some efforts in obtaining InGaN columnar nanostructures; in particular, we are interested in growing self-assembled nanocolumns (NCs).

## EXPERIMENTAL DETAILS

InGaN ternary alloys were grown in a Riber C21 molecular beam epitaxy system used to grow nitrides and arsenides with an ultimate base pressure of  $2 \times 10^{-10}$  torr. This machine is equipped with a radio frequency (RF) gas source for supplying ions and atoms of nitrogen from molecular form. A deflection system based on electrical potential integrated in this set-up guarantees the presence of only atomic nitrogen species involved in the growth. InGaN samples were synthesized on Si (111) substrate with a miscut of  $4^\circ$  toward to the plane (110). Prior to the growth, the substrate was chemically treated to remove the native silicon oxides and to form a low temperature fresh layer of oxides according to the procedure given in [7]. After that, the Si (111) was mounted on In-free sample holder and put it inside of the load lock MBE chamber and then transferred to the growth reactor. To remove the oxides layer, the substrate was degassed at a temperature of  $900^\circ\text{C}$  for 10 minutes. A nitridation step was followed by exposing the Si surface to nitrogen plasma at 150 W and 0.25 sccm in molecular flux (equivalent to a pressure in the growth chamber of  $4.1 \times 10^{-6}$  torr) for 5 minutes. The next step consisted in depositing an AlN layer for 30 minutes at a beam equivalent pressure (BEP) of  $3.9 \times 10^{-7}$  torr in the Al effusion cell; keeping the same temperature and plasma conditions. Then, substrate temperature was lowered up to  $400^\circ\text{C}$  and InGaN was grown by a lapse of 1 hour. In order to get N-rich growth for self-assembling nanocolumns, the N plasma was raised to 350 W with a molecular flux of 0.75 sccm (equivalent to a pressure of  $1.4 \times 10^{-5}$  torr in the main reactor); the BEP's of In-cell and Ga-cell were varied but keeping the same metal flux in each sample. Figure 1 show an scheme of the structures grown. All the growth stages were monitored *in-situ* by using reflection high-energy electron diffraction (RHEED). X-ray diffraction technique was employed to evaluate the structural properties of the InGaN samples. A Philips X-pert diffractometer with a  $\text{CuK}\alpha$  ( $\lambda = 1.5406\text{\AA}$ ) radiation. Surface imaging of the InGaN nanocolumns was performed by using scanning electron microscopy (SEM); the surface morphology images were taken with an Auriga 39-16 microscope from Carl Zeiss. Two types of detectors were used to SEM pictures: secondary electron (SE) and in-lens detectors.

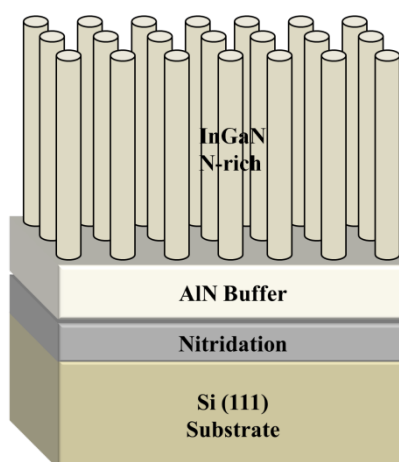


**Figure 1.** Schematic figure of the structures grown

## RESULTS AND DISCUSSION

Figure 2 shows top view micrographs of the final surfaces of some InGaN samples obtained by SEM and the corresponding RHEED patterns at the end of the growths (insets). In each image is indicated the sample ID and its respective concentration measured from XRD studies. In general, the RHEED patterns depict transmission characteristics; they are spotty with spots elongated along semicircles in all samples; indicating the growth of textured and slightly tilted polycrystalline InGaN films. In Figure 2(a) InN NCs are clearly seen; the NCs are vertically aligned with hexagonal shapes and flat surfaces. Three types of columns are identified: conical (diameters below 150 nm), cylindrical (diameters below 50 nm) and conical coalesced columns. InGaN micrographs show that the surface morphology is strongly dependent on the stoichiometry of In and Ga. In this case, SEM images exhibit different kind of topographies. In Figures 2(b) and 2(c), the samples 259 ( $\text{In}_{22.5}\text{Ga}_{77.5}\text{N}$ ) and 261 ( $\text{In}_{60.4}\text{Ga}_{39.6}\text{N}$ ), respectively, present a mixture between nanocolumns (diameters below 100 nm) and walls. Sample 263 ( $\text{In}_{47.5}\text{Ga}_{52.5}\text{N}$ ) in Figure 2(d) exhibits tilted tall walls and small grains. Detailed analysis based on side view SEM micrographs (not shown here) indicates that all topographies referred as walls are in many of them coalesced columns.

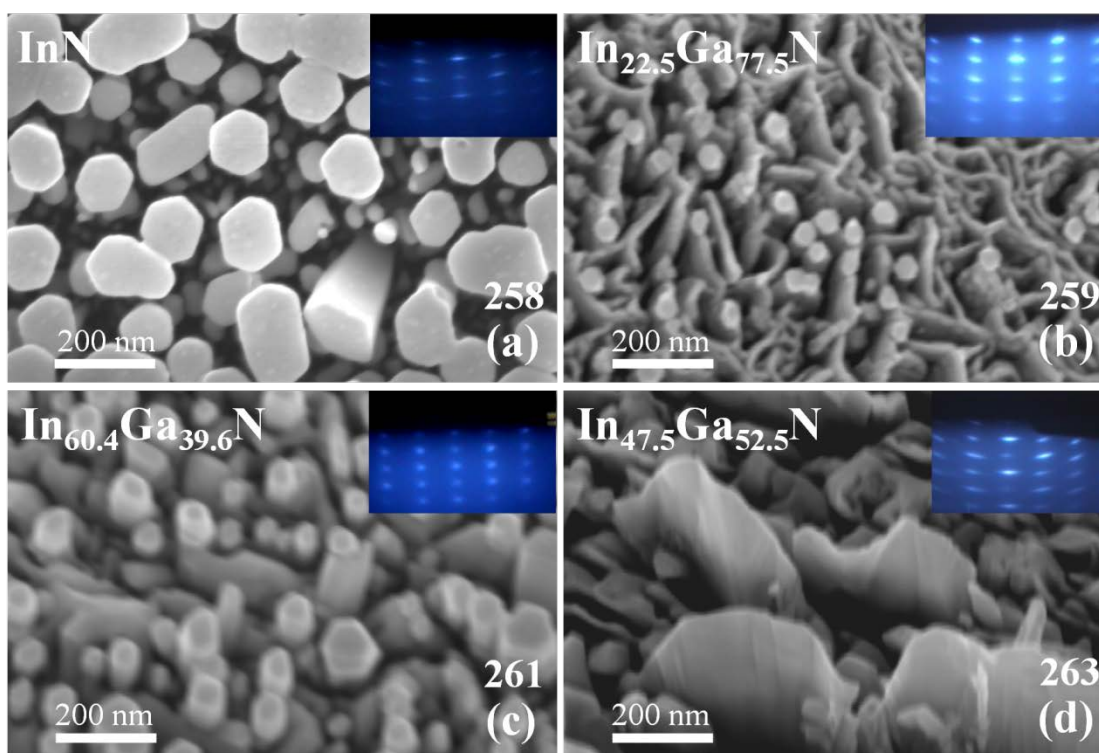


**FIGURE 2.** Top view SEM micrographs of the samples (a) 258, InN; (b) 259,  $\text{In}_{22.5}\text{Ga}_{77.5}\text{N}$ ; (c) 261,  $\text{In}_{60.4}\text{Ga}_{39.6}\text{N}$  and (d) 263,  $\text{In}_{47.5}\text{Ga}_{52.5}\text{N}$ . The concentrations were determined from XRD measurements. The inset in each SEM image corresponds to the RHEED pattern at the end of each growth.

Figure 3 displays the X-ray diffraction patterns for all samples grown measured in Bragg-Brentano geometry. Dashed lines corresponding to the positions of diffraction

peaks for Si(111), AlN(0002), GaN(0002) and InN(0002) deduced from the reported lattice parameters are drawn in the figure for comparison. The peak diffraction (0002) of the InGaN material is marked with an arrow. The existence of diffraction from (0002) planes of InGaN alloys guarantees their crystalline nature and hexagonal phase. Also, the different angular position of the InGaN peak in each sample ensures variation in composition from binary InN nanocolumns (sample 258) up to close GaN (sample 260) passing in middle concentrations (samples 262 and 263). In order to calculate the composition in the samples, we obtained the out-of-plane lattice parameters for all InGaN samples from XRD patterns and then, assuming a Vegard's law for those parameters, the concentration was estimated. Table 1 summarizes the results. Concentrations between 15 up to 60 % of In were calculated in InGaN ternary material.

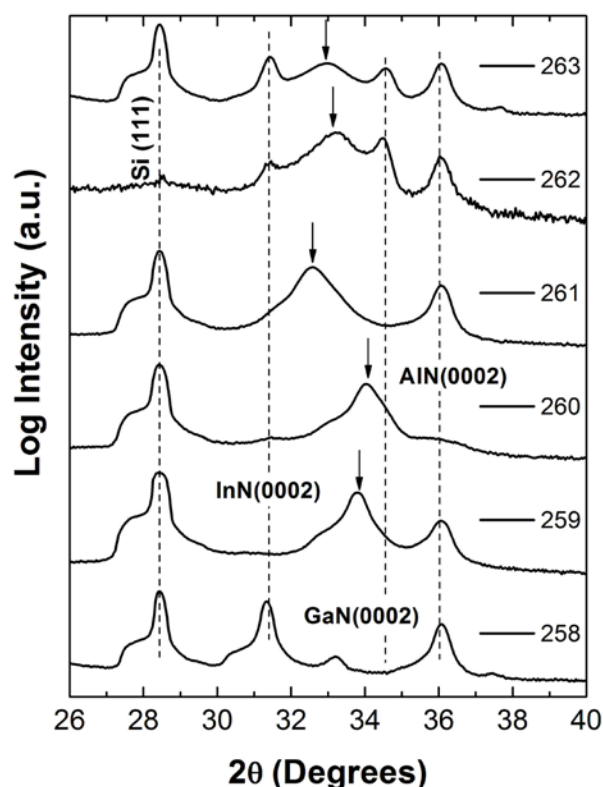


**FIGURE 3.** Diffractograms measured in the Bragg-Brantano configuration. The peak diffraction (0002) of InGaN alloys is marked with an arrow.

**TABLE 1.** Derived out-of-plane lattice parameters and compositions for all samples studied.

Sample ID	out-of-plane lattice parameter (nm)	Composition
258	0.570	InN
259	0.530	$\text{In}_{0.225}\text{Ga}_{0.775}\text{N}$
260	0.526	$\text{In}_{0.152}\text{Ga}_{0.848}\text{N}$
261	0.549	$\text{In}_{0.604}\text{Ga}_{0.396}\text{N}$
262	0.539	$\text{In}_{0.398}\text{Ga}_{0.602}\text{N}$
263	0.543	$\text{In}_{0.475}\text{Ga}_{0.525}\text{N}$

Separation of phases is observed in the XRD patterns in Figure 3; in particular, for samples 262 and 263 peaks assigned to the InGaN alloy and the separated InN and GaN components are clearly observed. This phenomenon was reported for the first time by Singh *et al* [8]. Due to large mismatch between InN and GaN (~ 11%), the observed phase separation is caused by strain related to the mixing of components highly mismatched in InGaN alloy. InGaN ternary material with high In content will separate into two phases with different In molar contents for reducing the strain energy of the system. Ho and Stringfellow calculated the phase diagram for InGaN system calculated using a modified valence-force-field model [9]. This diagram predicts that InGaN ternary alloy separates into two phases with different In compositions. According to this diagram, at a growth temperature of 400 °C, the alloy is immiscible practically in the whole range; therefore it is subjected to phase separation resulting in the binary compounds InN and GaN, as evidenced from XRD measurements in samples 261 and 262.

## CONCLUSIONS

Some efforts have been done in order to synthesize InGaN nanostructures by GSMBE under N-rich regime. At zero Ga-composition, InN NCs were grown successfully. XRD and SEM techniques exhibit the presence of InN NCs vertically aligned and relaxed. Regarding to the InGaN ternary material, in general, the samples present columnar features. Phase separation is observed at concentrations near 50 %, this result is explained in terms of immiscibility gap in the InGaN alloy.

## ACKNOWLEDGEMENTS

This work was partially supported by CONACyT-México and ICyTDF. The authors thank the technical assistance of R. Fragoso, M. Guerrero, E. Gómez, Z. Rivera, A. García, and A. Guillén.

## REFERENCES

1. T. Kuykendall, P. Ulrich, S. Aloni and P. Yang, *Nat. Mat.* **6**, 951-956 (2007).
2. Y. J. Hong, C.-H. Lee, A. Yoon, M. Kim, H.-K. Seong, H. J. Chung, C. Sone, Y. J. Park and G.-C. Yi, *Adv. Mater.* **23**, 3284-3288 (2011).
3. C. Hahn, Z. Zhang, A. Fu, C. H. Wu, Y. J. Hwang, D. J. Gargas and P. Yang, *ACS Nano* **5**, 3970-3976 (2011).
4. A. Khan, *Nat. Photon.* **3**, 432-434 (2009).
5. H.-W. Lin, Y.-J. Lu, H.-Y. Chen, H.-M. Lee and S. Gwo, *App. Phys. Lett.* **97**, 073101 (2010).
6. E. Matioli, C. Neufeld, M. Iza, S. C. Cruz, A. A. Al-Heji, X. Chen, R. M. Farrell, S. Keller, S. DenBaars, U. Mishra, S. Nakamura, J. Speck and C. Weisbuch, *App. Phys. Lett.* **98**, 021102 (2011).
7. A. Ishizaka and Y. Shiraki, *J. Electrochem. Soc.* **133**, 666-671 (1986).
8. R. Singh, D. Doppalapudi, T. D. Moustakas and L. T. Roman, *Appl. Phys. Lett.* **70**, 1089-1091 (1997).
9. I-h. Ho and G. B. Stringfellow, *Appl. Phys. Lett.* **69**, 2701-2703 (1996).